Construction and Building Materials 359 (2022) 129540

Contents lists available at ScienceDirect

Construction and Building Materials

journal homepage: www.elsevier.com/locate/conbuildmat

Double-life sustainable construction materials from alkali activation of volcanic ash/discarded glass mixture

Enrico Bernardo [a,*], Hamada Elsayed [a,b], Anna Mazzi [a], Giulia Tameni [a], Salvatore Gazzo [c], Loredana Contrafatto [c]

[a] Department of Industrial Engineering, University of Padova, Padova, Italy
[b] Refractories, Ceramics and Building Materials Department, National Research Centre, 12622 Cairo, Egypt
[c] Department of Civil Engineering and Architecture, University of Catania, Catania, Italy

ARTICLE INFO

Keywords:
Waste valorization
Alkali activation
Glass-ceramics
Cellular materials

ABSTRACT

Volcanic ash, according to the large amount of silica and alumina, may be considered as feedstock for geopolymers. However, the relatively low reactivity, mostly due to the relatively low amount of amorphous phase, implies the introduction of ash as minor component in complex mixtures and the activation with highly concentrated alkaline solutions. This paper aims at improving the sustainability of ash conversion into inorganic polymers with adequate strength-to-density ratio, by minimizing the addition of valuable compounds and including discarded material. Fine powders of volcanic ash from Mt Etna (Italy), in fact, were activated with NaOH solutions at low molarity (3 M), with a variable water/solid ratio (0.35–0.42), after mixing with waste glass powders, from cullet purification. The adopted ash/glass proportion (50 wt%-50 wt%) was intended to favour the reuse of inorganic polymers, by firing at 950 °C, in turn causing the transformation into porous glass-ceramics with a remarkable strength-to-density ratio. A significant foaming was effectively observed, due to decomposition of hydrated alkali alumino-silicates developed upon hardening. Foams with excellent strength-to-density ratio were also obtained by thermal transformation of highly porous cold consolidated materials.

1. Introduction

Mt Etna, located in the Italian island of Sicily, is the highest and one of the most active volcanoes of the Eurasian plate. During 2021, the eruptions occurred had considerable intensity and duration. Sixteen eruptive events occurred in the period from 16 February to the end of March. Large volumes of pyroclastic products covered the surrounding territory and urban areas on the slopes of the volcano, producing disruptive effects on transport systems. For each paroxysmal episode, quantities varying from about 30 to 600 kg/m^2 fell to the ground, affecting an area of over 1200 km^2 [1]. To avoid the inclusion of volcanic ash in the already wide range of inorganic waste, the application of volcanic material becomes imperative.

Circular economy represents a fundamental pillar for sustainable development targets: the mandatory claim “reduce, reuse, recycle” can answer to the global criticalities of waste increase and resources depletion [2]. To realize circularity actions avoiding dangerous burden shifting phenomena, consistent data and information are needed [3] and a life cycle perspective have to be adopted, in order to clarify the environmental responsibilities of processes including all the life cycle stages “from cradle to grave” [4]. In the last two decades, numerous studies have clarified the environmental profile associated with products and their end-of-life scenarios; however, sometimes recycle seems a downcycling rather than an upcycling solution [5].

The reuse of Etnean volcanic waste, as part of an end-of-waste strategy, has had a strong impulse in recent years [6]. Some studies have been addressed to the reuse in the field of mortar and concrete production [7] and lightweight insulating bio-plasters [8–10]. Other uses concern different end of waste alternative such as the production of ceramic tiles [11] and the synthesis of zeolite as adsorbent material in the field of water treatment [12]. All products are undoubtedly interesting, but an end-of-life perspective is missing.

A very significant research trend concerns the application of ashes for the development of geopolymers, although the selection of other precursors may be critical [13,14]. A first example of geopolymer concretes based on volcanic ash in alkaline solution was reported by Sontia

* Corresponding author.
E-mail address: enrico.bernardo@unipd.it (E. Bernardo).

https://doi.org/10.1016/j.conbuildmat.2022.129540
Received 20 June 2022; Received in revised form 4 September 2022; Accepted 19 October 2022
Available online 27 October 2022

Metekong et al. [15]. The approach was successful (operating at different curing temperatures, such as 28–60-80 °C), but it implied the use of concentrated sodium silicate and sodium hydroxide solutions (10 M) and addition of calcined laterite. Ash specifically from Mt Etna has been considered similarly, in formulations involving sodium hydroxide (8 M) and Na- or K- silicate, but also different amounts of metakaolin (from 5 to 25 wt%) [16,17]. Mixtures containing volcanic ash without any addition of metakaolin required thermal curing at 100 and 400 °C to complete the alkaline activation and to give satisfactory mechanical properties. Mt. Etna pyroclastic wastes were suggested as low cost building materials, suitable also for restoration of areas of cultural heritage damage, close to the volcanic site ("recycling at km 0") [16].

In general, the feasibility of geopolymerization reaction from volcanic ash without any additional reactive alumino-silicate is due to very concentrated alkaline solutions, not relying simply on hydroxides. As an example, Tchakoute et al. [18] produced geopolymer pastes cured at ambient temperature, with the support of 12 M sodium hydroxide and sodium silicate solutions. An alternative activation process consisted of the fusion method, performed in combination with sodium hydroxide, and addition of Al_2O_3 [18]. Djobo et al. [19], starting from Cameroonian volcanic ash, referred again to 12 M sodium hydroxide and sodium silicate solutions, observing a notable increase (~50 %) of the 28-day compressive strength in the case of the paste cured at 80 °C, for 24 h (about 30 MPa), compared to the paste cured at ambient temperature (about 20 MPa).

The direct activation with alkali hydroxides may represent an improvement, in terms of sustainability, by reducing synthesis costs, but it is still challenging. Kamseu et al. [20] recently underlined that solid precursors like volcanic ash and waste glass need significant amount of energy in the grinding into fine powders but necessitate very low volume of alkaline solution to be activated in the production of alkali activated materials. The simplicity of activation with NaOH solutions was confirmed by other authors [21,22]; again, an issue may be represented by the concentrations (at least 6 M).

The present paper is intended to offer a new strategy concerning the handling of volcanic ash from Mt. Etna. More precisely, it deals with the concept of waste glass useful in controlling both consolidation at nearly room temperature, with obtainment of inorganic polymers, after activation of fine powders in NaOH solutions at low molarity (3 M), and thermal transformation, at 950 °C, as an end-of-life option of the same inorganic polymers. In other words, the approach aims at developing sustainable materials with a 'double life', with dismantled components of a first generation possibly recycled into components of a second generation, as shown by Fig. 1.

The adopted waste glass consisted of the fraction of soda-lime glass resulting, in form of fine powders, as a residue of the purification of container glass cullet. Being enriched in contaminants (i.e. traces of polymeric and metallic materials), the fraction is discarded in landfills, rather than used in the manufacturing of new containers, by remelting (heterogeneous contaminations would impair the quality of new containers). The waste, however, may be considered as feedstock for new construction materials, in products involving viscous flow sintering at moderate temperatures (not exceeding 1000 °C, so well below the temperatures required by melting) [23], as well as in inorganic polymers. Fly ash based geopolymers, as an example, may be developed by using activating solutions based on NaOH, instead of Na silicate, according to the mixing of ashes with waste glass [24]. Interestingly, soda-lime waste glass may undergo a 'mild' activation, i.e. at low molarity (NaOH or KOH not exceeding 3 M), although the products cannot be fully classified as geopolymers, according to the formation of a 'tobermorite-like gel' (based on hydrated calcium silicate compounds), rather than 'zeolite-like gel' (hydrated alkali alumino-silicate) [23].

We will show that a volcanic ash/glass waste mixture (50 wt%-50 wt %) is particularly interesting for the above-mentioned 'double-life' potential. In fact, it actually yields zeolite-like gels, upon curing at nearly room temperature, but confirming previous studies on mixtures of volcanic material and soda-lime glass in the same proportion [25], it also supports the development of highly porous glass-based bodies. In the present case, the gas release is attributable the decomposition of hydrated phases developed upon consolidation at nearly room temperature. Finally, the porosity may be even enhanced by considering the transformation of already highly porous inorganic polymers, obtained by gas evolution during activation.

2. Materials and methods

2.1. Raw materials

The adopted volcanic ash (V) consisted of municipal waste removed from the public spaces after explosive eruptions of Mt. Etna during February 2021. The material had a code number 200303, according to the European Waste Catalogue (EWC). Waste glass powder (G) was provided by the company SASIL SpA (Biella, Italy) in the form of fine particles (mean particle size of 75 μm), corresponding to the glass fraction that remains practically unusable, after colour selection and removal of metallic and polymeric residues, due to the presence of ceramic contaminations. The chemical compositions of the starting materials (XRF analysis of volcanic ash courtesy of Buzzi Unicem SpA, Augusta, Italy; data on soda-lime glass from previous work [23]) are shown in Table 1.

Volcanic ash waste was dried in oven at the temperature of 110 °C for 6 h, crushed by a ball mill, and then sieved to 75 μm. No specific treatment or preliminary washing was carried out. The glass powder was used in the fraction below 75 μm. Commercial sodium hydroxide (99 % pure by mass, Marten Srl, Maierato, Italy), was used to prepare the alkaline activator. The sodium hydroxide solution with 3 mol/L (3 M) concentration was prepared by mixing the pure granular sodium hydroxide with distilled water. The solution was used immediately after preparation, without any cooling because no significant heat is developed due to its low molarity.

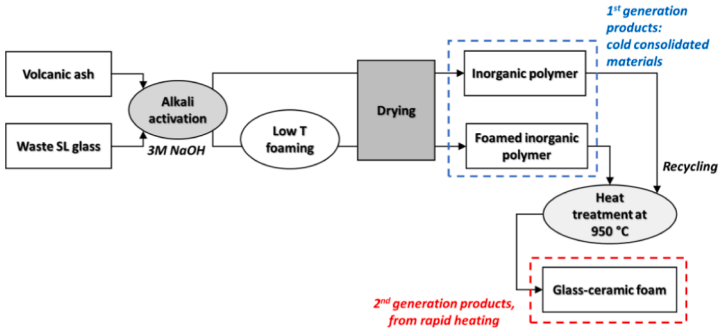

Fig. 1. Schematic of the adopted approach to volcanic ash/waste glass mixtures.

Table 1
Chemical analysis (oxide contents in wt%) of volcanic ash (V) and glass cullet (G).

	V	G
SiO_2	46.8	71.7
TiO_2	1.9	0.1
Al_2O_3	16.0	0.7
Fe_2O_3	11.9	0.1
MgO	6.3	3.3
CaO	9.8	10.1
Na_2O	2.8	13.2
K_2O	1.8	0.1
SO_3	0.3	0.2
Other	2.4	0.5

Three pastes with a different water-based solution-to-solid ratio (w/s) of 0.35, 0.39, 0.42 were prepared. The solid phase consisted of V and G in the 50 wt%-50 wt% proportion. V and G were preliminarily homogenized by dry mixing in the ball mill, at the speed of 450 rpm for 10 min. Pastes were later obtained by adding the sodium hydroxide solution and by mixing for 30 min at 450 rpm. The mixtures were labelled as V5G5_w/s.

The beginning of the setting time was for all the mixture about 20 min after the mixing of the sodium hydroxide solution and the powders started. After completing the mixing, lasting a total of 30 min, the fresh pastes were cast into three gang iron moulds of 40 mm × 40 mm × 160 mm, according to EN 196-1. Two moulds for each mixture were cast, for a total of six prismatic specimens per mixture type. The moulds were vibrated using a shaking table for about 2 min to remove air bubbles. Then the moulds containing the samples were coated with a thin film of polyethylene to avoid intensive water evaporation and then kept for 72 h in the oven at 75 °C (temperature used also for previous experiments on alkali activation of soda-lime glass, under 'mild' alkali activation [23]). The samples were then removed from the oven and after 24 h demoulded and immediately subjected to mechanical testing.

A mixture with w/s = 0.42 was considered also for room temperature foaming experiments. After mixing for 30 min at 400 rpm, the slurry was added with 1 wt% SPB (sodium perborate monohydrate,) and 1 wt% SDS (sodium dodecyl sulphate), referring to the weight of fine powders [26]. After additional stirring (at 1200 rom) for 5 s, the slurry was cast in closed polystyrene containers (diameter ~ 60 mm) and left at 75 °C for 72 h. After demoulding, thick discs were cut into blocks of approximately 15 mm × 15 mm × 15 mm, for subsequent operations.

Residues from mechanical testing (flexural tests) were cut and shaped into cubic blocks of approximately 15 mm × 15 mm × 15 mm by means of a diamond saw and a diamond polishing plate (100 μm finish). These blocks, together with some blocks from room temperature foaming, were subjected to heat treatment at 950 °C, by direct insertion in a muffle furnace, with a holding time of 15 min. At the end of the holding time, the samples were rapidly cooled, at approximately 60 °C/min, below 800 °C (with the muffle switched off and muffle door partially open), and then naturally cooled to room temperature (inside the muffle).

2.2. Characterization

The geometrical density (ρ_{geom}) of samples was computed from the weight-to-volume ratios on regular blocks, after careful determinations of weights and dimensions utilizing an analytical balance and a digital caliper. The apparent density (ρ_{app}) and the true density (ρ_{true}) were evaluated using a helium pycnometer (Micromeritics AccuPyc 1330, Norcross, GA, USA), operating on bulk or finely crushed samples, respectively. The measured density values were employed to calculate the amount of total, open, and closed porosity.

The flexural strength and compressive strength characterization on big samples was performed, according to the specification of EN 196-1 on cement testing. The flexural strength was obtained by carrying out three point bending test on the prismatic samples applying a linear ramp at the loading rate of 50 N/s ± 10 N/s until the specimen breaks. A steel frame equipped with a 5 kN load cell, connected to an HBM UPM 60 data acquisition system was used. The compressive strength tests were performed on the half-prisms resulting from the flexural breakage with the CONTROLS system composed by a 100 kN frame complete with pressure and strain transducer and connected to Advantest 9 computerised control console. A linear ramp at the loading rate of 2400 N/s ± 200 N/s was applied. The free shrinkage was evaluated as the linear dimensional variation of the prismatic test specimens following the method in EN 12617-4. Block from room temperature foaming underwent compressive tests, on at least 8 specimens, supported by an universal testing machine (Quasar 25, Galdabini S.p.a., Cardano al Campo, Italy), operating with a cross-head speed of 1 mm/min.

Thermally treated samples underwent gentle polishing, to achieve blocks again of 15 mm × 15 mm × 15 mm, later used for a second series of compressive tests, on at least 8 specimens for each sample type. Strength-density plot were computed according to experimental data and data for commercial building materials, by means of CES (Cambridge Engineering Selector) software package (Granta EduPack, Ansys Granta, Canonsburg, PA, USA).

The mineralogical analysis of finely powdered samples, before and after heat treatment, was performed by X-ray diffraction (XRD, Bruker D8 Advance, Karlsruhe, Germany – CuKα radiation, 0.15418 nm, 40 kV–40 mA, 2θ = 10–70°, step size 0.05°, 2 s counting time). The phase identification was supported by the Match! program package (Crystal Impact GbR, Bonn, Germany), on data from the PDF-2 database (ICDD-International Centre for Diffraction Data, Newtown Square, PA). The same samples were studied also by infrared spectroscopy (FTIR, FTIR model 2000, Perkin Elmer Waltham, MA, USA); spectra were recorded in the 4000–500 cm^{-1} range collecting an average of 64 scans with 2 cm^{-1} resolution.

3. Results and discussion

3.1. Activation of volcanic ash/soda lime glass mixture

Fig. 2 shows the X-ray diffraction pattern of volcanic ash from Mt. Etna in the starting condition. The above-mentioned limited sensitivity to alkali activation, due to the limited amorphous phase, is substantially confirmed, given the number of diffraction maxima, attributable to different silicates and alumino-silicates.

Interestingly, the detected silicate and alumino-silicate crystal phases presented much different degrees of polymerization of SiO_4 and AlO_4 units. The most intense peaks are attributable, as main crystal phase, to plagioclase [$Ca_{0.78}Na_{0.22}Al_{1.78}Si_{2.22}O_8$, PDF#89-1480], i.e. a solid solution between Ca feldspar (anorthite, $CaAl_2SiO_8$) and Na feldspar (albite, $NaAlSi_3O_8$) in a molar ratio of approximately 4:1. Such phase can be classified as a framework alumino-silicate, defined by the full connection between SiO_4 and AlO_4 tetrahedra, the latter being stabilized by alkali and alkaline earth ions [27]. Other very intense peaks were attributed to a complex pyroxene solid solution [$Ca_{0.79}Al_{0.06}Fe_{0.08}Mg_{0.47}Fe_{0.60}Si_2O_6$, PDF#74-2425] (Al- and Mg-containing variant of hedenbergite $CaFeSi_2O_6$), possessing a chain structure involving SiO_4 tetrahedra connected by means of two of the four oxygens [28]. In addition, we could not exclude the presence of olivine [$Mg_{1.215}Fe_{0.785}SiO_4$, PDF#76-0551], featuring isolated SiO_4 units [29].

The addition of glass obviously determined a 'dilution' of silicate and alumino-silicate crystal phases and an increase of amorphous phase. The adopted soda-lime glass actually featured quartz [SiO_2, PDF#89-1961] and calcite [$CaCO_3$, PDF#86-2334] contaminations.

The alkali activation determined substantial changes, shown by the top pattern in the same Fig. 2, for w/s = 0.42. Given the height of the characteristic peaks, not substantially decreased by comparison of the activated mix with the dry mix, the feldspar phase did not practically

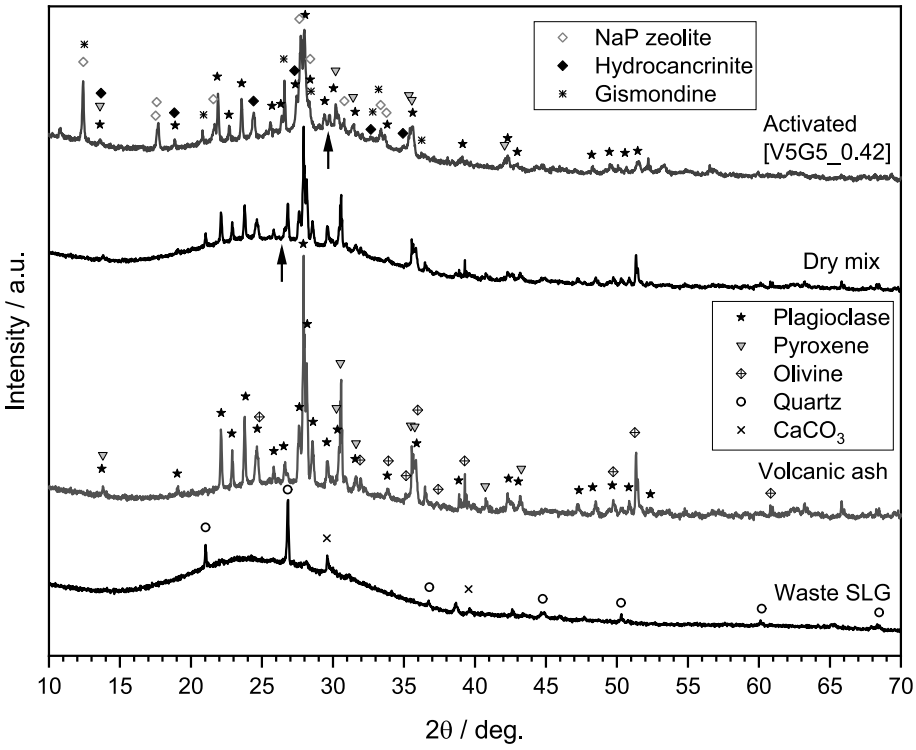

Fig. 2. X-ray diffraction analysis of volcanic ash and soda-lime glass, in as received state, in dry-mixed state and after activation [w/s = 0.42].

dissolve. On the contrary, silicates with less interconnected structure evidently reacted. The dissolution of olivine, in alkali solution, is in good agreement with the literature [30].

The interaction with the activating solution involved also the amorphous material. The 'hump' resulting from the 'amorphous background' of soda-lime glass and amorphous phase of volcanic ash, initially centered at 2θ ~ 26° (see the arrows marked in Fig. 2), in the dry mix of VA and GP, had a substantial 'upshifting' (the new center being at 2θ ~ 29.5°), consistent with the precipitation of N-A-S-H gel [31]. In addition, many diffraction maxima indicate newly formed phases, mainly in the form of Na-based zeolites, such as zeolite NaP [$Na_8(Al_8Si_8O_{32})(H_2O)_{15.17}$, PDF#89–6322] and hydrocancrinite [$Na_8Al_6Si_6O_{24}(OH)_2{\cdot}2H_2O$,PDF#46–1457]. The quite surprising increase of the diffraction peak at 2θ ~ 27°, attributed to quartz, is likely attributable to the overlapping with the diffraction signals of gismondine [$CaAl_2Si_2O_8{\cdot}4H_2O$, PDF#20–0452] (a Ca-based zeolite).

The possibility of developing inorganic polymers, from soda-lime glass waste, in relatively 'weak' alkaline solutions (e.g. 3 M KOH), had been already reported, according to Cyr and coworkers [32,33]. Due to the practical absence of Al_2O_3 in soda-lime glass, the hardening of

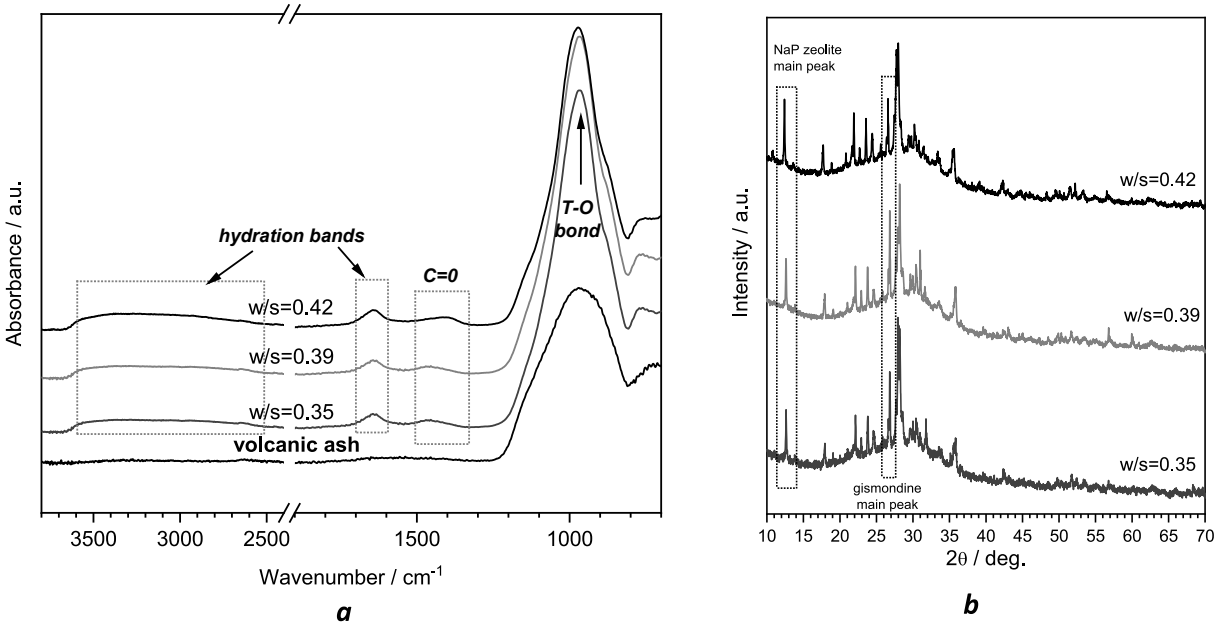

Fig. 3. Effect of w/s ratio on phase evolution, assessed by means of infrared spectroscopy (a) and X-ray diffraction analysis (b).

suspensions relied on the development of 'tobermorite-like gels', i.e. gels based on calcium silicate hydrated compounds, forming layered structures [34]. In the present case, with soda lime glass combined with volcanic ash, the presence of zeolite crystals cannot be seen as a proof of the development of a three-dimensionally interconnected zeolite-like gel (network determined by the bridging of SiO_4 and AlO_4 units [35]) matrix, but the superior stability could be easily assessed, at first, by immersion in boiling water. For samples from activated volcanic ash/glass mixtures, in fact, no disintegration or dissolution was observed.

The formation of a zeolite-like gel was evidenced by infrared spectroscopy, as illustrated by Fig. 3a. Independently from the amount of activating solution (leading to different w/s ratios), for hardened volcanic ash/glass mixtures the band at 950–960 cm^{-1}, attributable to the asymmetric stretch of T–O bonds, corresponding to oxygen connected with Al or Si ions, appear much more pronounced than in the starting volcanic ash. Hydration bands (2500–3600 cm^{-1} and 1600–1700 cm^{-1}, corresponding to O—H stretching and bending, respectively) are also visible. Finally, very weak signals, at 1430 and 1470 cm^{-1}, could be due to traces of carbonate compounds [23].

The comparison of diffraction patterns for different w/s ratios, shown in Fig. 3b, reveals slight changes, in the peaks at $2\theta \sim 12.5°$ and $2\theta \sim 27°$. NaP zeolite, having a stronger line at $2\theta \sim 12.5°$, was likely favored at high w/s (more liquid brought more NaOH), whereas gismondine, with a stronger line at $2\theta \sim 27°$, was favored at low w/s.

3.2. Morphology and mechanical properties of cold-cnsolidated bodies

All samples, after drying, were homogeneous and crack-free. As shown by Fig. 4a, there was no macropore; the quite abundant residual porosity came from the packing of adjacent unreacted particles, shown in Fig. 4b, bound by semi-crystalline gel. As demonstrated by Fig. 4c, unreacted particles derived both from glass (darker colour) and volcanic ash (lighter colour; in backscattered electron images lighter colors are attributed to particles including heavier elements).

Operating with w/s = 0.42, suspensions had a very fluid consistency and showed a significant bleeding phenomenon during the vibration of the moulds. The elimination of water, with drying, did not correspond to a significant shrinkage; on the contrary, the shrinkage remained very limited (1.12 %), accompanied by abundant porosity (>35 vol%). Such condition was quite surprising, since a general feature of alkali-activated binders is the more pronounced shrinkage compared to cement-based mortars, due the fact that water does not incorporate directly in the production of alumino-silicate gel and remains, in a small volume, as interstitial water [36].

As pointed out by Ascensao et al. [37] the shrinkage in inorganic polymers is governed by complex, overlapping phenomena, such as autogenous shrinkage and dry shrinkage. The first derives from the difference between the absolute density of the reaction products and the starting materials, whereas the second is defined by the progressive emptying of the initially saturated pore structure with progression of reaction. The mechanisms are severely affected by the reactivity of precursors and water amount, and they are associated with internal stresses, e.g. dry shrinkage forces the pore structure to a severe inward contraction. We can posit that our particular precursors, in the particular reaction conditions (mould sealed with thin plastic film) formed a rigid network, which could withstand the drying-induced stresses.

The reduction of w/s did not affect shrinkage and porosity linearly. A slight decrease of w/s (to 0.39) led to advantages in the processing, consisting of improved workability, fluid-to-plastic consistency and scarce bleeding, but enhanced the shrinkage and the overall porosity in the final products. A significant decrease of w/s (to 0.35), on the contrary, led to poor workability but reduced the shrinkage (<1 %) and the overall porosity.

As reported by Table 2, the different w/s ratios led to quite variable mechanical properties, reasonably conditioned by the above-mentioned internal stresses. The best trade-off of flexural and compressive strength with low density was achieved with V5G5_0.42 samples; in any case, all the developed materials matched well with widely recognized lightweight construction materials, such as Plaster of Paris and structural lightweight concrete, in terms of both compressive strength and flexural strength, as illustrated by the charts in Fig. 5a and Fig. 5b, respectively. It is interesting to note that Plaster of Paris and structural lightweight concrete are excellent references: for the given density range, they are 'non-dominated' solutions, i.e. they represent the strongest solutions (in the charts, the best trade-offs of high strength and low density

Table 2
Physical and mechanical properties of samples from activated mixture of volcanic ash and soda lime glass.

Sample type	V5G5_0.35	V5G5_0.39	V5G5_0.42	V5G5_0.42 foam
Density (g/cm^3)	1.58 ± 0.02	1.51 ± 0.02	1.58 ± 0.02	0.65 ± 0.01
Total porosity (TP, vol%)	31.7 ± 0.1	38.2 ± 0.1	36 ± 0.1	74.1 ± 0.1
Open porosity (OP, vol%)	29.3 ± 0.1	37.5 ± 0.1	35.5 ± 0.1	73.9 ± 0.1
Closed porosity (CP, vol%)	2.4 ± 0.1	0.7 ± 0.1	0.5 ± 0.1	0.2 ± 0.1
Linear shrinkage (%)	0.92 ± 0.4	2.78 ± 0.2	1.42 ± 0.6	n.a.
Flexural strength (MPa)	5.9 ± 1.1	4.5 ± 0.4	4.9 ± 1.5	n.a.
Compressive strength (MPa)	15.8 ± 0.9	16.6 ± 0.9	17.9 ± 1.7	0.9 ± 0.1

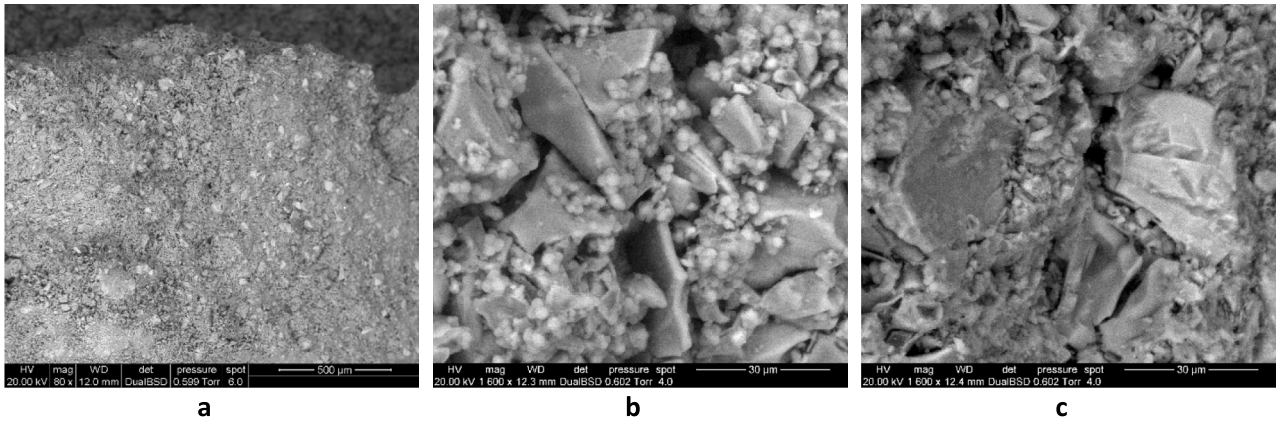

Fig. 4. Microstructural details of V5G5_0.42sample at increasing magnification.

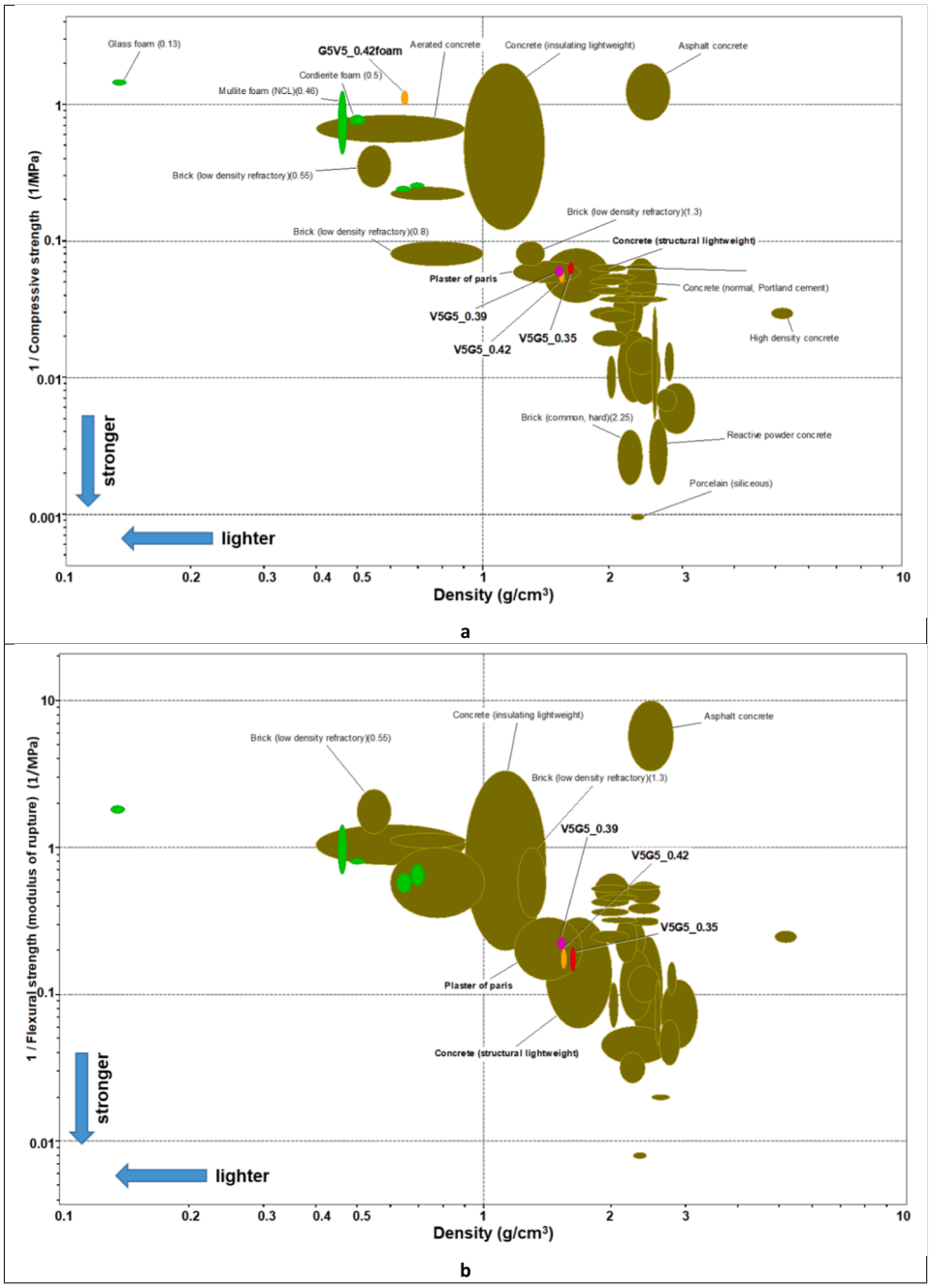

Fig. 5. Strength/density trade-offs, for the comparison of developed materials with commercial products: a) compressive strength; b) flexural strength (computed by means of CES software package).

correspond to points close to the bottom left corner).

3.3. *Effect of heat treatment*

As previously stated, the obtainment of inorganic polymers was a primary, but not exclusive objective. In the perspective of the reuse of inorganic polymers, we referred to a past investigation on foams from powders of glass combined with volcanic material (basalt 'scoria') [25]. In the field of inorganic products for thermal and acoustic insulation, a well-established solution is represented by glass foams. Such foams are generally produced by gas evolution in a pyroplastic mass, in turn defined by viscous flow sintering of glass powders (at 900–1000 °C) with concurrent gas evolution, resulting from powder additives (carbon black, SiC, calcium carbonate) [23,38]. Iron-rich volcanic materials, combined with soda-lime glass, are actually 'self-foaming': intensive foaming may be observed according to the reduction of ferric oxide (involving Fe^{3+} ions) into ferrous oxide (involving Fe^{2+} ions), with oxygen release [25]. The mixtures actually underwent oxidation upon heating above 700 °C (with Fe^{2+} passing to Fe^{3+}), followed by reduction at 1100 °C. Although fired at higher temperature than glass foams, the products were interesting for the partial crystallization, in turn enhancing the mechanical properties. The proportion between volcanic material and glass waste, adopted also in the present investigation (50 wt%-50 wt%), had led to optimized foams, reasonably due to a favourable balance between viscous flow, promoted by the glass fraction, and crystallization, promoted by volcanic material.

Using a mixture of volcanic material and glass, after alkali activation, instead of a mixture of powders, was reputed as an important advantage.

The compounds developed upon alkali activation (such as zeolite crystals), in fact, could act as 'internal' foaming agents, by simple dehydration, reasonably occurring well below those required for the reaction involving iron oxides. The heat treatment at only 950 °C was suggested to explore the foaming in the usual temperature range adopted for commercial glass foams [38].

Fig. 6 shows that cold consolidated materials effectively turned into cellular bodies, by firing at 950 °C. There was a substantial increase of porosity, still mostly open, as reported in Table 3. As illustrated by the chart in Fig. 7, the samples exhibited a promising trade-off between (compressive) strength and density; in particular, the samples were comparable to lightweight refractory bricks. With reference to lightweight concrete, they feature comparable strength, but with much lower density; the higher specific strength of the new cellular bodies suggests their use as new lightweight aggregates.

The increase of porosity was substantial, but not as dramatic as observed with previous studies on direct heating of basalt scoria/glass mixtures (leading to bodies with > 85 % total porosity, at 1100 °C). The limited foaming may be justified also by the crystallization. As shown by Fig. 6c, cell walls effectively exhibited a multitude of tiny, fibrous crystals. In general, the foaming of glasses is greatly complicated by the crystallization, since it greatly increases the viscosity of pyroplastic masses realized by the sintering of softened glass powders. Significant foaming may be obtained with limited crystallization [38].

Rigid inclusions were not attributable to the crystal phases already present in the volcanic ash or in the products from cold consolidation of ash/glass mixtures. As expected, zeolite phases decomposed; more interestingly, plagioclase (present in volcanic ash and nearly unreacted upon alkali activation) practically disappeared, as shown by Fig. 8a. We can posit that both glass softening and decomposition of zeolites contributed to the formation of liquid phase, which dissolved the plagioclase and later turned into a glass–ceramic, featuring new crystal phases embedded in a glass matrix.

The most intense diffraction peaks are attributable to wollastonite [$CaSiO_3$, PDF#84–0654], accompanied by a new pyroxene solid solution [$Ca_{1.007}(Mg_{0.805}Fe_{0.214})(Si_{1.75}Fe_{0.241})O_6$, PDF#89–0835] and traces of the previously detected plagioclase. The crystallization increased with increasing w/s ratio (w/s = 0.42), as testified by Fig. 8b (see the enhanced intensity of diffraction peaks). One possible explanation is the enhanced sodium intake from the activation solutions, since alkali-rich glasses feature a lower activation energy for crystal growth [39].

The observed compressive strength data are in good agreement with the development of a glass–ceramic matrix. For an open-celled solid, the compressive strength σ_c typically follows the well-recognized Gibson-Ashby model [40], which predicts an exponential correlation with the relative density (ratio between geometric and true densities, ρ_{rel}=(100-TP)/100; TP is the total porosity):

$\sigma_c \sim 0.2 \cdot \sigma_{bend} \cdot (\rho_{rel})^{1.5}$.

where σ_{bend} is the bending strength of the solid phase, in a pore-free condition. For the V5G5_0.42 fired sample (featuring the highest total porosity and the lowest amount of closed porosity) the observed compressive strength of 4.3 ± 0.5, could be correlated to a bending strength of the solid phase well exceeding 150 MPa, typical for glass-ceramics [27].

Table 3
Physical and mechanical properties of samples from activated mixture of volcanic ash and soda lime glass, after firing.

Sample type	V5G5_0.35	V5G5_0.39	V5G5_0.42	V5G5_0.42 foam
Density (g/cm^3)	0.75 ± 0.02	0.72 ± 0.03	0.68 ± 0.01	0.37 ± 0.01
Total porosity (TP, vol %)	72.1 ± 0.1	72.4 ± 0.1	74.5 ± 0.1	86.2 ± 0.1
Open porosity (OP, vol %)	63 ± 0.1	64.8 ± 0.1	71.6 ± 0.1	81.8 ± 0.1
Closed porosity (CP, vol%)	9.1 ± 0.1	7.6 ± 0.1	2.9 ± 0.1	4.4 ± 0.1
Compressive strength (MPa)[Bending strength of solid phase (MPa)]	4.6 ± 0.6	4.5 ± 0.5	4.3 ± 0.5 [~170]	2.0 ± 0.4 [~190]

3.4. Low temperature foaming: 'green' and fired cellular bodies

Slurries from alkali-activated suspensions may yield highly porous foams, according to mechanical and chemical methods. The mechanical foaming implies intensive stirring of suspensions ('direct foaming') at the early stages of gelation [23]. Air bubbles are first incorporated, with the help of surfactants, and then stabilized by the progressive gelation. Chemical foaming, for the sake of simplicity, may be realized just by addition of compounds releasing gas at the early stages of reaction [26], with surfactants introduced again to stabilize the gas/liquid interface and prevent any coalescence of gas bubbles.

As illustrated by Fig. 9a, a slight amount of sodium perborate, combined by SDS surfactant, sufficed in determining a significant expansion in a sample from w/s = 0.42 (G5V5_0.42 – foamed). As shown by Fig. 5a, the new foam was quite weaker than the other samples from cold consolidation; the compressive strength, however, was still in the range observed for lightweight (thermally insulating) concrete, with a much lower density.

A remarkable improvement in compressive strength occurred with the thermal treatment at 950 °C, for 15 min. The firing determined, again, the transformation into glass–ceramic foams. No change was

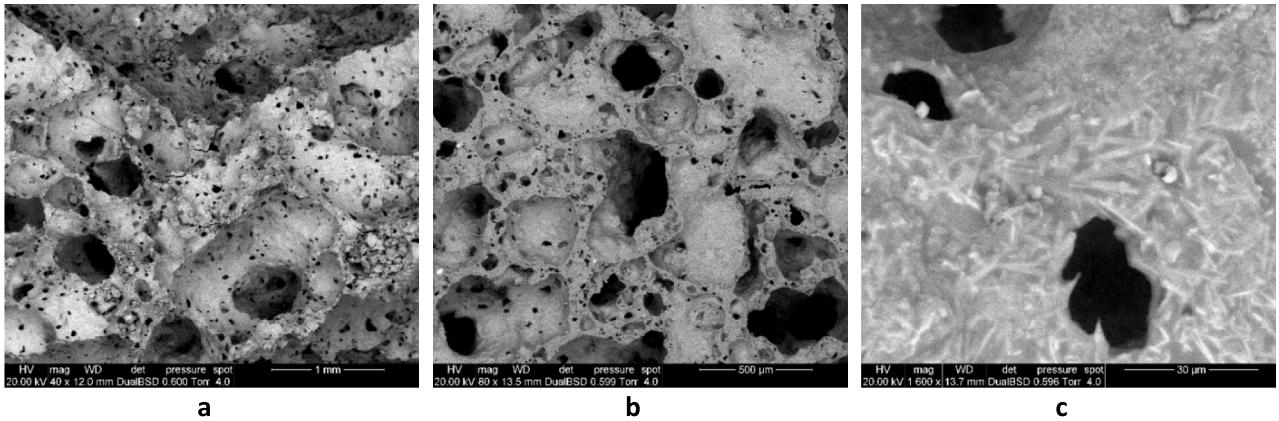

Fig. 6. Microstructural details of selected fired samples: a) V5G5_0.35; b,c) V5G5_0.42.

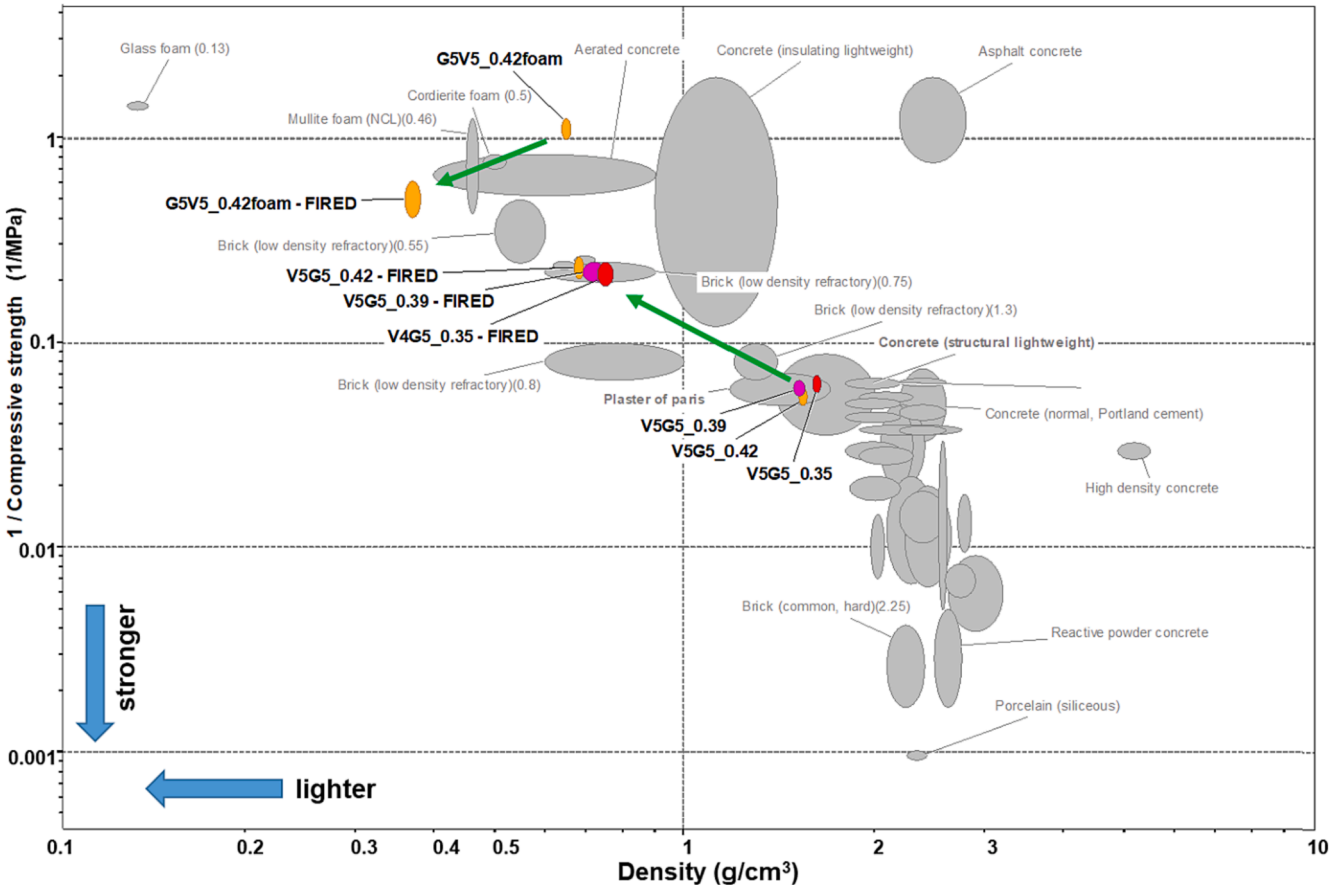

Fig. 7. Compressive strength/density trade-off of fired products (computed by means of CES software package).

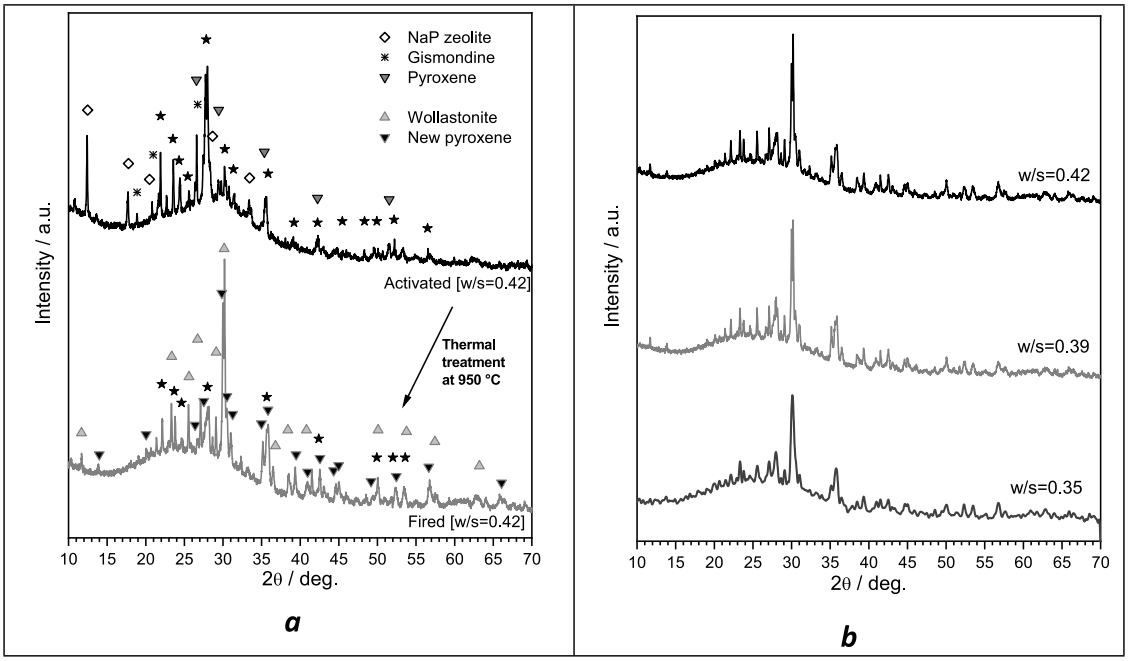

Fig. 8. Transformation of gels with heat treatment at 950 °C (a) and effect of w/s ratio on crystallization (b).

observed in the phase assemblage, compared to the previous fired sample from w/s = 0.42, according to diffraction analysis (not shown). Fig. 7 illustrates that firing led to a foam had a strength-to-density ratio well exceeding that of commercial mullite- and cordierite-based foams. The excellence of the last glass–ceramic foams is also testified by the computation of the bending strength of the solid phase (~200 MPa, see Table 2).

In conclusion, the studied mixture of volcanic ash and waste glass

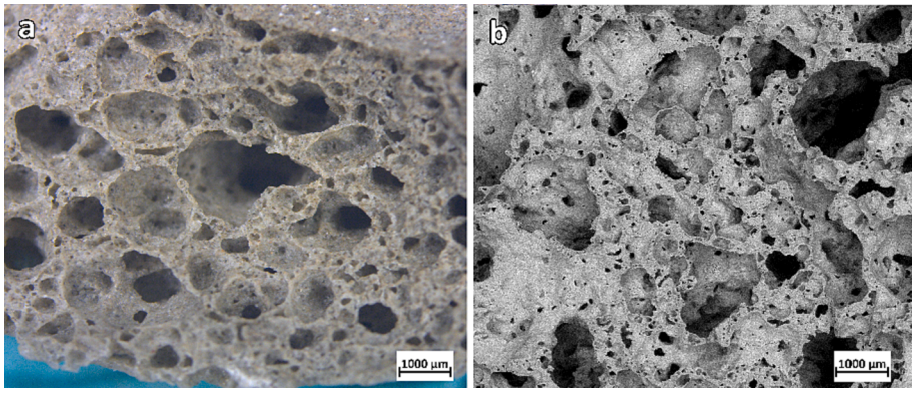

Fig. 9. Microstructure of V5G5_0.42foam sample before (a) and after (b) heat treatment.

offers a remarkably wide range of applications. The direct activation with 3 M NaOH solution generally offers lightweight components, comparable to existing Portland cement-based ones; the low temperature foaming just operates a 'switch' from products more oriented to load-bearing applications to products more oriented to thermal insulation. The conversion into glass-ceramics, after heat treatment (suggested also as recycling option for products from alkali activation), implies, in all cases, the definition of components possibly coupling load resistance and thermal insulation.

4. Conclusions

Volcanic ash from Mt. Etna expressed a great potential for the obtainment of multiform new building materials, according to alkali activation in combination with soda-lime glass. The sustainability is substantiated by two key facts: i) lightweight inorganic polymers may be obtained by activation with NaOH solution of low molarity; ii) the developed inorganic polymers have an end-of-life option, since they may be considered as precursors for porous glass-ceramics, in turn having a potential, in constructions, as lightweight aggregates. The approach of 'double life' products may be further extended, by definition of highly porous inorganic polymers, possibly transformed into glass–ceramic foams with excellent strength-to-density. Future efforts will undoubtedly involve the exploration of different setting conditions, different volcanic ash/glass proportions and different types of discarded glasses.

CRediT authorship contribution statement

Enrico Bernardo: Conceptualization, Investigation, Methodology, Software, Supervision, Writing – review & editing, Funding acquisition. **Hamada Elsayed:** Investigation, Data curation. **Anna Mazzi:** Writing – review & editing, Funding acquisition. **Giulia Tameni:** Investigation, Data curation, Writing – original draft. **Salvatore Gazzo:** Investigation, Data curation. **Loredana Contrafatto:** Conceptualization, Investigation, Methodology, Supervision, Writing – review & editing.

Declaration of Competing Interest

The authors declare that they have no known competing financial interests or personal relationships that could have appeared to influence the work reported in this paper.

Data availability

The authors do not have permission to share data.

Acknowledgements

Enrico Bernardo and Anna Mazzi acknowledge the funding from the University of Padova (Dept. of Industrial Engineering), in the framework of the "SusPIRe" (Sustainable porous ceramics from inorganic residues, BIRD202134). E.B., H.E. and G.T. acknowledge the support of national project MUR PON R&I 2014-2021. The authors thank Dr. Patricia Rabelo Monich (University of Padova, currently at Denmark Technical University) Mr. Michele Garbari (University of Padova), and Mr. Enrico Mangano, Eng., (University of Catania) for experimental assistance.

References

[1] Reports of the National Institute of Geophysics and Volcanology (INGV) - https://www.ct.ingv.it/index.php/monitoraggio-e-sorveglianza/prodotti-del-monitoraggio/comunicati-attivita-vulcanica (accessed 20 June 2022).
[2] J. Korhonen, A. Honkasalo, J. Seppälä, Circular economy: The concept and its limitations, Ecol. Econ. 143 (2018) 37–46, https://doi.org/10.1016/j.ecolecon.2017.06.041.
[3] H. Salmenperä, K. Pitkänen, P. Kautto, L. Saikku, Critical factors for enhancing the circular economy in waste management, J. Clean. Prod. 280 (2021), 124339, https://doi.org/10.1016/j.jclepro.2020.124339.
[4] A. Mazzi, Introduction. Life cycle thinking. In: J. Ren, S. Toniolo (Eds), Life Cycle Sustainability Assessment for Decision-Making: Methodologies and Case Studies. Elsevier, ISBN: 9780128183557, 1-19. 10.1016/B978-0-12-818355-7.00001-4.
[5] D. Reike, W.J.V. Vermeulen, S. Witjes, The circular economy: new or refurbished as CE 3.0? – Exploring controversies in the conceptualization of the circular economy through a focus on history and resource value retention options, Res. Cons. Recycling 135 (2018) 246–264, https://doi.org/10.1016/j.resconrec.2017.08.027.
[6] REUCET Project Report: Recovery and reuse of Etna volcanic ash. Editor Prof. P. Roccaro, CSISA, Catania, Italy, February (2021), ISBN 88-7850-024-0.
[7] L. Contrafatto, Recycled Etna volcanic ash for cement, mortar and concrete manufacturing, Constr. Build. Mater. 151 (2017) 704–713, https://doi.org/10.1016/j.conbuildmat.2017.06.125.
[8] L. Contrafatto, C. Lazzaro Danzuso, S. Gazzo, L. Greco, Physical, mechanical and thermal properties of lightweight insulating mortar with recycled Etna volcanic aggregates, Constr. Build. Mater. 240 (2020), 117917, https://doi.org/10.1016/j.conbuildmat.2019.117917.
[9] L. Contrafatto, S. Gazzo, A. Purrazzo, A. Gagliano, Thermo-mechanical characterization of insulating bio-plasters containing recycled volcanic pyroclasts, Open Civ. Eng. J. 14 (2020) 66–77, https://doi.org/10.2174/1874149502014010066.
[10] L. Contrafatto, M. Cuomo, S. Gazzo, L. Greco, A. Purrazzo, Meso-scale prediction of insulating mortar thermal properties, Lect. Notes Mech. Eng. (2020) 1190–1199, https://doi.org/10.1007/978-3-030-41057-5_97.
[11] C.M. Belfiore, C. Amato, A. Pezzino, M. Viccaro, An end of waste alternative for volcanic ash: a resource in the manufacture of ceramic tiles, Constr. Build. Mater. 263 (2020), 120118, https://doi.org/10.1016/j.conbuildmat.2017.06.125.
[12] C. Belviso, M. Abdolrahimi, D. Peddis, E. Gagliano, M. Sgroi, A. Lettino, P. Roccaro, F.G.A. Vagliasindi, P.P. Falciglia, G. Di Bella, M.G. Giustra, F. Cavalcante, Synthesis of zeolite from volcanic ash: characterization and application for cesium removal, Microporous Mesoporous Mater. (2021), 111045, https://doi.org/10.1016/j.micromeso.2021.111045.
[13] M. Nawaz, A. Heitor, M. Sivakumar, Geopolymers in construction – Recent developments, Constr. Build. Mater. 260 (2020), 120472, https://doi.org/10.1016/j.conbuildmat.2020.120472.
[14] L. Contrafatto, Volcanic Ash, In: R. Siddique, R. Belarbi (Eds.), Sustainable Concrete Made with Ashes and Dust from Different Sources: Materials, Properties and Applicationc, Elsevier Book (2021), ISBN: 978-0-12-824050-2. 10.1016/B978-0-12-824050-2.00011-5.
[15] J.V. Sontia Metekong, C.R. Kaze, J.G. Deutou, P. Venyite, A. Nana, E. Kamseu, U. C. Melo, T.T. Tatietse, Evaluation of performances of volcanic-ash-laterite based blended geopolymer concretes: Mechanical properties and durability, J. Build. Eng. 34 (2021), 101935, https://doi.org/10.1016/j.jobe.2020.101935.

[16] C. Finocchiaro, G. Barone, P. Mazzoleni, C. Leonelli, A. Gharzouni, S. Rossignol, FT-IR study of early stages of alkali activated materials based on pyroclastic deposits (Mt. Etna, Sicily, Italy) using two different alkaline solutions, Constr. Build. Mater. 262 (2020), 120095, https://doi.org/10.1016/j.conbuildmat.2020.120095.
[17] G. Barone, C. Finocchiaro, I. Lancellotti, C. Leonelli, P. Mazzoleni, C. Sgarlata, A. Stroscio, Potentiality of the use of pyroclastic volcanic residues in the production of alkali activated material, Waste Biomass Valorization 12 (2) (2021) 1075–1094, https://doi.org/10.1007/s12649-020-01004-6.
[18] H. Tchakoute Kouamo, J.A. Mbey, A. Elimbi, B.B. Kenne Diffo, D. Njopwouo, Synthesis of volcanic ash-based geopolymer mortars by fusion method: Effects of adding metakaolin to fused volcanic ash, Ceram. Intern. 39 (2) (2013) 1613–1621, https://doi.org/10.1016/j.ceramint.2012.08.003.
[19] J.N. Yankwa Djobo, A. Elimbi, H. Kouamo Tchakouté, S. Kumar, Mechanical properties and durability of volcanic ash based geopolymer mortars, Constr. Build. Mater. 124 (2016) 606–614, https://doi.org/10.1016/j.conbuildmat.2016.07.141.
[20] E. Kamseu, V. Alzari, D. Nuvoli, D. Sanna, I. Lancellotti, A. Mariani, C. Leonelli, Dependence of the geopolymerization process and end-products to the nature of solid precursors: Challenge of the sustainability, J. of Clean. Prod. 278 (2021), 123587, https://doi.org/10.1016/j.jclepro.2020.123587.
[21] P.N. Lemougna, K.J.D. MacKenzie, U.F.C. Melo, Synthesis and thermal properties of inorganic polymers (geopolymers) for structural and refractory applications from volcanic ash, Ceram. Int. 37 (8) (2011) 3011–3018, https://doi.org/10.1016/j.ceramint.2011.05.002.
[22] S. Zhou, C. Lu, X. Zhu, F. Li, Upcycling of natural volcanic resources for geopolymer: comparative study on synthesis, reaction mechanism and rheological behavior, Constr. Build. Mater. 268 (2021), 121184, https://doi.org/10.1016/j.conbuildmat.2020.121184.
[23] A. Rincón, G. Giacomello, M. Pasetto, E. Bernardo, Novel 'inorganic gel casting' process for the manufacturing of glass foams, J. Eur. Ceram. Soc. 37 (2017) 2227–2234. http://ddoi.org/10.1016/j.jeurceramsoc.2017.01.012.
[24] N. Toniolo, A. Rincón, J.A. Roether, P. Ercole, E. Bernardo, A.R. Boccaccini, Extensive reuse of soda-lime waste glass in fly ash-based geopolymers, Constr. Build. Mater. 188 (2018) 1077–1084, https://doi.org/10.1016/j.conbuildmat.2018.08.096.
[25] M. Marangoni, M. Secco, M. Parisatto, G. Artioli, E. Bernardo, P. Colombo, H. Altlasi, M. Binmajed, M. Binhussain, Cellular glass–ceramics from a self foaming mixture of glass and basalt scoria, J. Non Cryst. Solids 403 (2014) 38–46, https://doi.org/10.1016/j.jnoncrysol.2014.06.016.
[26] L. Korat, V. Ducman, Characterization of fly ash alkali activated foams obtained using sodium perborate monohydrate as a foaming agent at room and elevated temperatures, Front. Mater. 7 (2020), https://doi.org/10.3389/fmats.2020.572347.
[27] W. Höland, G. Beall, Glass-Ceramic Technology; The American Ceramic Society: Westerville, OH, USA, 2002.
[28] M. Day, F. Hawthorne, A structure hierarchy for silicate minerals: Chain, ribbon, and tube silicates, Mineral. Mag. 84 (2020) 165–244, https://doi.org/10.1180/mgm.2020.13.
[29] A.M. Escatllar, T. Lazaukas, S.M. Woodley, S.T. Bromley, Structure and properties of nanosilicates with olivine $(Mg_2SiO_4)_N$ and pyroxene $(MgSiO_3)_N$ composition, ACS Earth Chem. 3 (2019) 2390–2403, https://doi.org/10.1021/acsearthspacechem.9b00139.
[30] B. Traynor, C. Mulcahy, H. Uvegi, T. Aytas, N. Chanut, E.A. Olivetti, Dissolution of olivines from steel and copper slags in basic solution, Cem. Concr. Res. 133 (2020), 106065, https://doi.org/10.1016/j.cemconres.2020.106065.
[31] I. Garcia-Lodeiro, E. Aparicio-Rebollo, A. Fernández-Jimenez, A. Palomo, Effect of calcium on the alkaline activation of aluminosilicate glass, Ceram. Int. 42 (2016) 7697–7707, https://doi.org/10.1016/j.ceramint.2016.01.184.
[32] M. Cyr, R. Idir, T. Poinot, Properties of inorganic polymer (geopolymer) mortars made of glass cullet, J. Mater. Sci. 47 (2012) 2782–2797, https://doi.org/10.1007/s10853-011-6107-2.
[33] R. Idira, M. Cyr, A. Pavoine, Investigations on the durability of alkali-activated recycled glass, Constr. Build. Mater. 236 (2020) 117–477, https://doi.org/10.1016/j.conbuildmat.2019.117477.
[34] J.S. Dolado, M. Griebel, J. Hamaekers, A molecular dynamic study of cementitious calcium silicate hydrate (C–S–H) gels, J. Am. Ceram. Soc. (2007) 3938–3942, https://doi.org/10.1111/j.1551-2916.2007.01984.x.
[35] J.L: Provis,, Geopolymers and other alkali activated materials: why, how, and what? Mater. Struct. 47 (2014) 11–25, https://doi.org/10.1617/s11527-013-0211-5.
[36] M. Mastali, P. Kinnunen, A. Dalvand, R. Mohammadi Firouz, M. Illikainen, Drying shrinkage in alkali-activated binders – A critical review, Const. Build. Mater. 190 (2018) 533–550, https://doi.org/10.1016/j.conbuildmat.2018.09.125.
[37] G. Ascensao, G. Beersaerts, M. Marchi, M. Segata, F. Faleschini, Y. Pontikes, Shrinkage and mitigation strategies to improve the dimensional stability of CaO-FeO_x-Al_2O_3-SiO_2 inorganic polymers, Mater. 12 (2019) 3679, https://doi.org/10.3390/ma12223679.
[38] E. Bernardo, G. Scarinci, P. Bertuzzi, P. Ercole, L. Ramon, Recycling of waste glasses into partially crystallized glass foams, J. Porous Mater. 17 (2010) 359–365, https://doi.org/10.1007/s10934-009-9286-3.
[39] T. Watanabe, H. Hashimoto, M. Hayashi, K. Nagata, Effect of alkali oxides on crystallization in CaO–SiO_2–CaF_2 glasses, ISIJ Int. 48 (2008) 925–933, https://doi.org/10.2355/isijinternational.48.925.
[40] Gibson, L.J.; Ashby, M.F., Cellular Solids, Structure and Properties, 2nd edition, Cambridge University Press, 1999, Cambridge, UK.